Does the 2007 Noto Hanto earthquake reveal a weakness in the Japanese national seismic hazard map that could be remedied with geological data?

Shinji Toda and Yasuo Awata

Active Fault Research Center, Geological Survey of Japan, AIST, site 7, 1-1-1 Higashi Tsukuba, Ibaraki 305-8567, Japan

(Received June 29, 2007; Revised February 12, 2008; Accepted February 25, 2008; Online published November 7, 2008)

The Noto Hanto earthquake struck one of the lowest earthquake probability regions on the national seismic hazard map of Japan. To contribute to future updates of the hazard map, we examined the predictability of the 2007 earthquake on the basis of geological data that were available before it occurred. Sonic prospecting profiles of active faulting and the absence of an onshore fault could have limited the potential rupture length to 12–15 km, similar to the 2007 source. Empirical relationships between magnitude and fault length would have given us $M_j = 6.6$–6.8 and $M_w = 6.3$–6.4. The emergence of one marine terrace, which inclines to the south and reaches an altitude of approximately 50 m, can be dated to 120–130 ka and yields an uplift rate of approximately 0.4 mm/year. M_w-displacement empirical relationships and examples of recent blind fault events that have occurred at various locations around the world suggest that the conceivable maximum coseismic uplift of such shocks is 40–70 cm. Together with the uplift rate, we would have obtained an average recurrence interval of 1000–2000 years and, consequently, a 1.5–3.0% time-independent (Poisson) probability for 30 years. In addition, the significant inclination of the marine terraces—3.2 per mille (0.32%)—is better explained by the accumulation of frequent southward tilting as large as that of the 2007 type event with approximately 1600-year intervals, without any significant contributions from other seismic sources. We therefore conclude that the Noto Hanto earthquake source would have been better evaluated and identified if we had taken into account not only major active faults but also the active tectonics of moderate-size faults and their associated scale and rate.

Key words: Noto Hanto earthquake, blind thrust, earthquake probability, seismic hazard map, long-term earthquake forecasting.

1. Introduction

The Earthquake Research Committee of the Headquarters for Earthquake Research Promotion (subsequently referred to as ERC), a special governmental organization of Japan, released the probabilistic national seismic hazard maps in March 2005. These are based on 10 years of intensive surveys of paleoseismic trenches, drillings, and seismic recordings and the assemblage of existing seismic and geological data dating from after the 1995 Kobe shock (Fig. 1; ERC, 2005). Because of the short recurrence times and time-dependence of subduction earthquakes (e.g. the next Tokai earthquake is considered to be imminent), the coastal regions facing the Pacific Ocean have high probabilities—higher than 26% in the next 30 years—of experiencing earthquakes with JMA seismic intensity (I_{jma}) $\geq$ VI (equivalent to MMI X–XI) or lower. In contrast, inland regions, such as those facing the Japan Sea, have the lowest probabilities due to the infrequent activity of shallow, large active faults. In fact, one may argue that the ERC forecasting map has already failed because several recent destructive earthquakes, recorded at $I_{jma} \geq$ VI, or lower, have struck the lower probability areas along the Japan Sea (Fig. 1). The 2007 Noto-Hanto earthquake is one such example.

The national hazard map is largely based on the maximum size of regional earthquakes and their frequencies, focusing on subduction zones and major active faults longer than 20 km. In terms of predicting the frequency of destructive earthquakes, the map displays the fundamental weakness of the ERC's evaluation system because it ignores short-length active faults inland that are associated with active folds, crustal tilting, and ocean bottom active faults near coastlines. In order to revamp the evaluation system to incorporate such minor and faint but numerous shallow earthquake sources, it is important to use all existing geological data available.

In this paper, we first review the mechanism of the source fault of the Noto Hanto earthquake. We then seek correlations with active geological and geomorphological features and retrospectively forecast the Noto Hanto earthquake, estimating its magnitude, recurrence interval, and probability.

2. Overall Relationship between Geological Structure, Source Fault, and Aftershocks

From north to south, the Noto Peninsula is composed of the NE-trending Oku-Noto Hill, N-trending Chu-Noto Hill, and NE-trending Sekido Range (Fig. 2). This range and hills are composed of inclined crustal blocks bounded by transverse geological faults and offshore and inland NE-

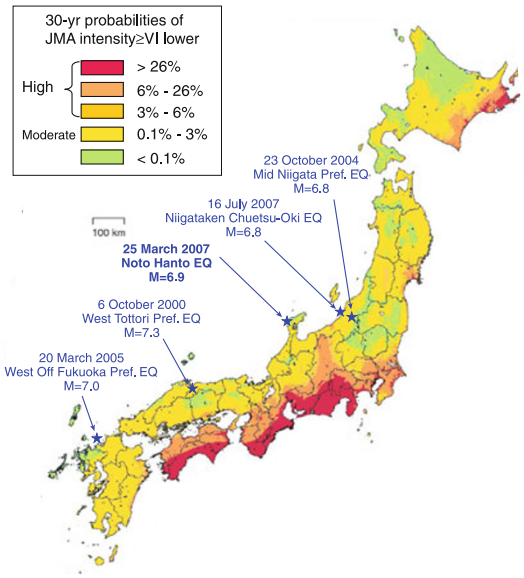

Fig. 1. Probabilistic seismic hazard map of Japan for strong ground motion of JMA intensity = VI lower and greater for the next 30 years starting from 2005 (Earthquake Research Committee of the Headquarters for Earthquake Research Promotion, 2005), and recent destructive shallow earthquakes recorded by JMA with intensity ≥ VI or lower. Note that all five shocks occurred where the 30-year probabilities are lower than 3%; the 2007 Noto Hanto earthquake struck in one of the lowest earthquake probabilistic regions.

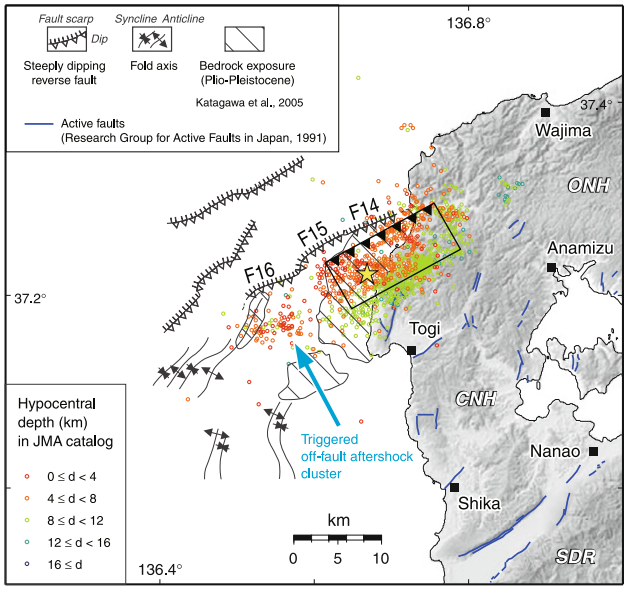

Fig. 2. Noto Hanto aftershocks within the first 24 hr, and mapped active structure on and off the Noto Peninsula. Star denotes the epicenter. Thick black square with teeth marks is the surface projection of the source fault modeled by Awata *et al.* (2008). Aftershocks are from JMA PDE catalog. ONH, Oku-Noto Hill; CNH, Chu-Noto Hill; SDR, Sekido Range.

trending faults that have been active since the late Tertiary period (e.g. Ota and Hirakawa, 1979). WNW-oriented compressional strain detected by the GPS networks (Sagiya *et al.*, 2000) provides evidence of the driving force for both NE- and N-trending faults despite the low strain rate relative to the other regions in Japan. The 2007 Noto Hanto earthquake occurred at the structural junction of the Oku-Noto and Chu-Noto Hills. The fault plane solution of the Noto Hanto earthquake (JMA, 2007; NIED, 2007; USGS, 2007) suggests that the earthquake was caused by a steeply dipping reverse fault with a right-lateral component, which is consistent with a slip oblique to the maximum compressional stress axis. The aftershock distribution within the first day, which generally shows a source fault dimension, suggests an approximately 15-km-long reverse fault (Fig. 1).

The onshore region is mainly underlain by the Miocene sedimentary and volcanic rocks (Geological Survey of Japan, 1992). Although there are approximately 2-km-wavelength NE-trending folds (Geological Survey of Japan, 1967), no evidence is currently available indicating either the presence of active folds or mapped faults associated with the eastern part of the 2007 source (Ota *et al.*, 1976; Research Group for Active Faults in Japan, 1991). In contrast, Okamura (2003) and Katagawa *et al.* (2005) reported the presence of several active faults in the offshore region from their sonic prospecting surveys west of the Peninsula. Katagawa *et al.* (2005) in particular detailed a couple of NE-trending inclined and uplifted blocks bounded by a group of active faults, a part of which corresponds to the mainshock and aftershock zone of the Noto Hanto earthquake. Following a detailed correlation study between onshore geology and acoustic stratigraphy, these researchers interpreted the tilted block as originating in the Neogene Tertiary to upper Quaternary. Based on fault linearity, discontinuity, and the timing of the most recent movements, they subdivided the block bounding the fault into three sub-faults, F14, F15, and F16, and active folds further west (Fig. 2). They also speculated that the sub-fault F14 possibly offset the lower Holocene but is terminated by the upper Holocene, whereas the sub-faults F15 and F16 show no deformation of both Holocene periods and even older strata formed during the last glacial period. The aftershock zone within the first 24 hr, which is often used as a proxy for the source fault area, corresponds to the sub-fault F14 and eastern half of F15 (Fig. 2). Thus, paleoseismic evidence explains why the rupture of the Noto Hanto earthquake stopped roughly between sub-faults F14 and F16.

3. Source Constraint and Repeatability: Relationship between Coseismic Vertical Displacement and Long-term Deformation

The Noto Hanto earthquake caused significant coseismic crustal uplift (Geographical Survey Institute (GSI), 2007). Coastal uplift across the epicentral zone was visible after the earthquake and provided information that was more useful in determining the coseismic deformation than that recorded by the sparsely distributed GPS stations (note that InSAR analysis by GSI provides the best coseismic deformation, but it took about 2 weeks after the mainshock to obtain this analysis). Awata *et al.* (2008) measured the uplift on a preseismic shoreline composed of an emerged oys-

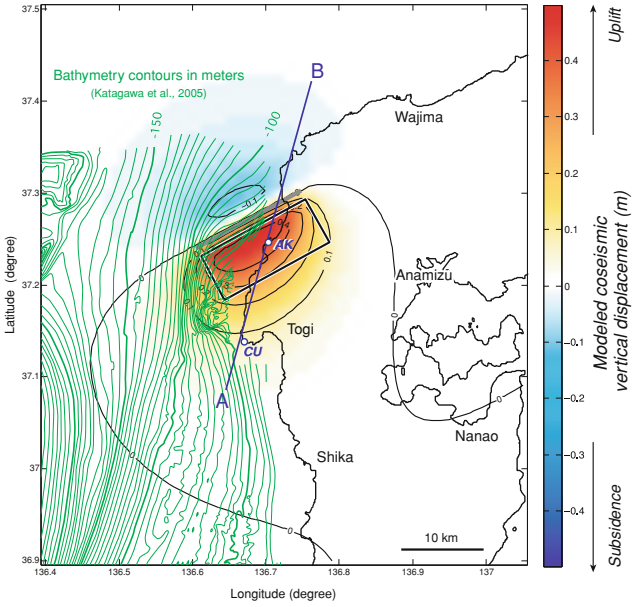

Fig. 3. Map showing a superb agreement between the western margin of the coseismically uplifted dome (gradational color) and curved bathymetric contours (green lines, with 5-m contour interval) formed by the protruded shelf atop the Noto Hanto source fault. The source fault is the black-lined rectangle. The blue A–B line is for a cross section shown in Fig. 4. AK and CU are Akakami and Chinoura, respectively, used for discussion in text.

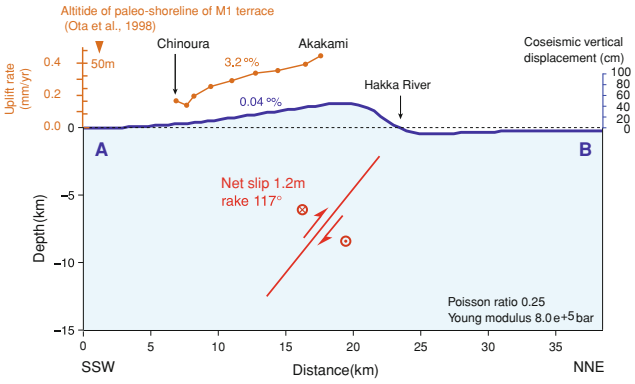

Fig. 4. Deformation profile of coseismic vertical displacement of the 2007 event (blue) and the former shoreline of the M1 terrace (orange) along the coastline (azimuth N16°E) that crosses the 2007 source fault. Coseismic deformation due to the 2007 event is calculated from a source fault model by Awata *et al.* (2008) that is denoted by red text and red lines. The marine terrace M1 resembles the coseismic deformation.

ter assemblage, algae, and other inter-tidal species along an approximately 50-km-long coastline between Wajima and Hakui. A maximum uplift of approximately 40 cm was measured between Tsurugiji and Akakami, 3–5 km NE of the epicenter, and a small subsidence of less than several centimeters was located between Fukami and Yoshiura, 13–17 km northeast of the epicenter. To explain the observed large uplift and the faint subsidence, these researchers modeled a steeply dipping blind reverse faulting that generates an asymmetric folding pattern at the Earth's surface. The spatial pattern shows a NE-trending concentric elliptic dome. Together with the bathymetric contours drawn by Katagawa *et al.* (2005), we found that the contour curvatures coincide with the westward convex shape of the coseismic uplift contours (Fig. 3). In other words, the coseismically uplifted area indeed corresponds to the widely distributed shallow shelf protruding to the west from the coastline. We believe this is not a coincidence but instead suggests that similar repeated earthquakes built the shallow shelf atop the 2007 source. The sonic prospecting profiles also furnish evidence that the uplifted shelf exposes Miocene and Paleogene Tertiary bedrocks (Katagawa *et al.*, 2005).

A widely distributed emerged marine terrace provides another source of compelling evidence for the repeatability of the 2007-type events. Ota (1975) and Ota *et al.* (1998) classified and mapped several stages of marine terraces and measured the former shorelines on the Noto Peninsula. The ages of the terrace groups are mostly unconstrained due to scanty dating material. However, the most widely and well-preserved M1 marine terrace is confirmed to have been formed during the maximum transgression of the Last Interglacial stage (marine oxygen isotope stage 5e), dated 120–130 ka. In and around the epicenter, the distribution of the M1 terrace is almost continuous from Akakami to Togi (Ota *et al.*, 1998). Altitudes of the former shorelines associated with the M1 terrace decrease from approximately 50 m at Akakami to approximately 20 m at Chinoura (Fig. 4). Since the older shorelines show greater height differences between Akakami and Chinoura, as Ota (1975) suggested, the block-tilting movement may have been continuous from the late Tertiary to the last interglacial stage, which is consistent with the speculation from offshore geology (Katagawa *et al.*, 2005). Coseismic coastal uplift due to the Noto Hanto earthquake shows a similar pattern of southward inclination along the coastline from Akakami to Chinoura (Awata *et al.*, 2008). Since the approximately 3.2 per mille slope of the M1 terrace is so steep, it is unlikely that other distant and large events have produced such significant tilting. Also, because the M1 landform can be simply built by successive 2007-sized coseismic uplifts, we interpret the 2007 Noto Hanto earthquake to be a characteristic event in this region and infer that earthquakes of its size and mechanism were the main contributors to the block uplift and inclination of the terraces.

4. Retrospective Forecasting Magnitude, Recurrence Time, and Probability

We assume that the magnitude of the Noto Hanto earthquake would have been evaluated from existing geological data even though there was no known remarkable active fault mapped prior to the earthquake (e.g. Research Group for Active Faults in Japan, 1991). As described above, fault F14 (discovered by Katagawa *et al.*, 2005) underlies the shelf to the coastline, with a length estimated to be 12–15 km (F14 is measured to be as long as 12 km in their paper, but due to the linearity between F14 and F15, most of fault F15 may be connected to F14, which extends the length to 15 km). If one had applied an empirical relationship between the M_j and fault length (Matsuda, 1975), the expected M_j would have been 6.6–6.8. If the Wells and Coppersmith (1994) formulae on M_w and subsurface rupture length for reverse fault had been used, we would have

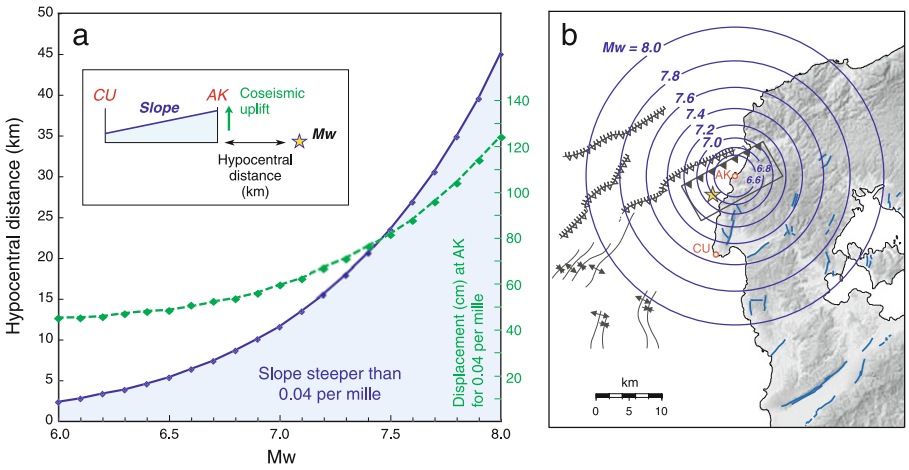

Fig. 5. All possible seismic sources that could have tilted the marine terraces in late Quaternary. (a) Hypocentral distance and M_w to reproduce a coseismic tilt steeper than 0.04 per mille (0.004%) between two locations separated by 11 km in an elastic half space. The light-blue area indicates the conditions for such a steep slope. (b) Theoretical locations of seismic sources and M_w to satisfy the conditions in (a). See Fig. 2 for geological legend.

an estimated M_w of 6.3–6.4. Because the Wells and Coppersmith formulae are derived using a global dataset obtained from different tectonic settings, we believe that the application of these formulae may slightly underestimate reverse faults in Japan. Further, the length of subsurface rupture is generally longer than that of a surface fault. In any case, both estimates are slightly smaller than the 2007 event but comparable in terms of earthquake damage and strong ground motion.

Assuming the characteristic earthquake hypothesis (Schwartz and Coppersmith, 1984) under stable tectonic loading, a combination of coseismic displacement D (mm) and long-term slip rate S (mm/year) allows us to estimate an average recurrence interval T_r (year) using the following simple equation (Wallace, 1970)

$$T_r = \frac{D}{S}. \tag{1}$$

Although it is impossible to measure D for a blind thrust fault, we suppose there are two possible approaches to estimating D beforehand. The first approach is to implement an empirical relationship between M_w and D_{max} for reverse faults associated with the recent earthquakes around the globe (table 2B in Wells and Coppersmith, 1994). Had we considered $M_w = 6.3$–6.4, we would have obtained $D_{max} =$ 97–104 cm from the following equation,

$$\log(D_{max}) = -1.84(\pm 1.14) + 0.29(\pm 0.17)M_w. \tag{2}$$

A caveat of this approach is that the variance from the regression curve for M_w and D_{max} shown in parentheses is fairly large (see also figures 10 and 11 in Wells and Coppersmith, 1994). $M_w = 6.3$–6.4 may consequently introduce a large range of D_{max} values (1 cm to 175 m) and, therefore, considerable errors. In reality, for reverse faults, since D_{max} represents net slip, it is necessary to convert the net slip to vertical displacement with conceivable dip angles. If we simply opt for a range of dip angles between 30° and 60° we obtain vertical displacement $DU_{max} = 49$–90 cm. The second approach is to directly approximate D from examples of similar blind thrust events. Several recent well-recorded earthquakes ranging from M_w 6.5 to 6.7 caused a maximum coseismic uplift of roughly 50 cm. For example, leveling surveys across the epicentral area of the 2004 mid-Niigata prefecture (Japan) earthquake ($M_j = 6.8$, $M_w = 6.6$) shows approximately 70 cm of maximum uplift at the anticline axis (GSI, 2004). The 1983 $M_w = 6.5$ Coalinga (California) earthquake recorded a vertical displacement of as much as 50 cm (Stein and Ekstrom, 1992). The 1994 $M_w = 6.7$ Northridge (California) earthquake upraised the Santa Susana Range over 40 cm (Hodgkinson *et al.*, 1996). Thus, we could have empirically assumed that a blind thrust event raised the Earth's surface 40–70 cm at most. For the Noto Hanto case, using an uplift rate S of 0.4 mm/year at Akakami and Tsurugiji (Fig. 3) and a conceivable coseismic vertical displacement of 40–70 cm, which is typical for a blind thrust, we could have obtained an average recurrence interval T_r of 1000–2000 years.

The uplifted M1 terrace with a slope of 3.2 per mille also supports the frequent occurrence of a Noto Hanto-type event that consequently produced a slope of 0.04 per mille (approx. 40 cm/11 km). Assuming the 2007 event is indeed characteristic, to contribute to the significant block tilting, one can estimate approximately 80 events since the last interglacial stage (approx. 125 ka) simply dividing 3.2 per mille by 0.04 per mille. This yields an average inter-event time of approximately 1600 years, which is consistent with that inferred from the uplift rate. However, one may argue that other possible sources could have contributed to the tilting. Here, we theoretically examine how large and how far other possible sources should be located to produce a slope steeper than 0.04 per mille using the equation (Okada, 1992)

$$\log U_{ave} = 1.5M_w - 2\log R - 6.6, \tag{3}$$

where U_{ave} (cm) is the expected average displacement due to an earthquake of moment magnitude M_w at the hypocentral distance R (km). Considering the maximum difference in simulated U_{ave} at both Akakami (AK) and Chinoura

(CU), we can examine the slope angle as a function of M and R. To obtain a slope as steep as 0.04 per mille, for example, sources of $M_w = 6.6$, 7.0, and 7.4 should be located closer than 6, 12, and 20 km, respectively (Fig. 5(a)). Since no such long faults within 10–20 km of Akakami actually exist (Fig. 5(b)), we can rule out the possibility that other seismic faults contribute directly to the production of the tilted M1 terrace. If remote large earthquakes had contributed to the uplift itself, but not the tilting, the inter-event time of the Noto Hanto type should be shorter than approximately 1600 years to maintain the slope.

Since we do not have any reliable paleoseismic information on the most recent large earthquake in the epicentral area, we cannot calculate a time-dependent conditional probability. However, assuming the characteristic earthquake hypothesis, $T_r = 1000$–2000 years, allows us to calculate a 1.5–3.0% time-independent (Poisson) probability for 30 years, which is comparable to the probabilities associated with the most active faults defined by ERC (compare: one quarter of the all known major active faults in Japan have time-dependent probabilities larger than 3%).

5. Discussion and Conclusion

The source fault of the March 25, 2007 Noto Hanto earthquake is located beneath both onshore and offshore portions of the northwest Noto Peninsula. No obvious onshore surface rupture accompanied the earthquake, but a significant vertical coseismic uplift of up to 40 cm was involved. Inland and off-shore geological data, ocean bottom topography, and uplifted marine terraces provide us with clues that enable us to retrospectively forecast the location of the source, the possible magnitude of the earthquake, and the recurrence interval (= earthquake probability). An up to 3% probability that an earthquake of $M_j = 6.6$–6.8 ($M_w = 6.3$–6.4) would occur in 30 years could have been forecasted at the Noto Hanto epicentral region if one had used all available data for the evaluation. This is quite unlike the approach used by ERC (2005) to construct their earthquake map of Japan, which takes into account only large earthquakes on long major active faults.

Abundant aftershocks have been recorded along the ENE-striking block-bounding faults, F14, F15, and F16 (Toda, 2008). Focal mechanisms of the moderate-sized aftershocks also suggest that the faulting mechanisms are consistent with the geological structure (figure 2 in Toda, 2008). However, as shown in the most recent tectonic landform and geological profiles obtained from sonic prospecting, there is no clear evidence that such faults and folds (western part of F-15, F16, and N-S-trending folds, etc.) produced any significant deformation during the Holocene. Accordingly, we may interpret the data as indicating that these faults are now inactive with respect to a large earthquakes but that they still react to the coseismic stress changes due to the mainshock and generate small- to moderate-sized earthquakes (Toda, 2008).

Is it appropriate to assume the characteristic earthquake hypothesis for such blind thrust events of moderate size? This question is critical and can introduce uncertainty into the evaluation of seismic risk in regions where both active faults and folds coexist. Even for the 2007 Noto Hanto case, our study shows evidence of both surface-cutting events and significant folding events. It is rational to conclude that the 2007 event justified the evaluation of fault activity by Katagawa *et al*. (2005). However, the criterion used in their study to identify the most recent activity consisted of a traditional approach to dating the timing and horizon of the fault upper termination, which practically contradicts the blind reverse faulting of the Noto Hanto earthquake. One can argue that there may have been larger events that offset the bottom of the sea floor in the past. Because the fault length is limited in the Noto case, we assume here that surface-cutting process may have occurred only rarely in 2007-type events.

Finally, what are the implications of this earthquake for the strategy of the long-term earthquake forecasting caused by hidden active faults ('gray zone fault'; Okumura, 2005) and offshore faults, which were not incorporated into the ERC strategy? We have indeed seen that the most recent destructive events were associated with shallow M 6 class earthquakes that did not expose any evident surface rupture. Perhaps what is most important is to use all available geological and geodetic off-fault information associated with the volumetric extent of the deformation as well as the one-dimensional on-fault data. Further, we have to properly evaluate the frequency of M 6 events in each region as well as the probabilities of the maximum size events that ERC have already calculated.

Acknowledgments. We wish to thank Hideki Katagawa, Yuichi Sugiyama, Ross Stein, and an anonymous reviewer for their helpful comments and discussion. We are also grateful to JMA and NIED for the hypocenter list.

References

Awata, Y., S. Toda, H. Kaneda, T. Azuma, H. Horikawa, M. Shishikura, and T. Echigo, Coastal deformation associated with the 2007 Noto Hanto earthquake, central Japan, estimated from uplifted and subsided intertidal organisms, *Earth Planets Space*, **60**, this issue, 1059–1062, 2008.

Geographical Survey Institute, The Mid Niigata prefecture Earthquake in 2004 report index: Results from leveling and GPS-observation, http://www.gsi.go.jp/WNEW/PRESS-RELEASE/2004/1227-1.jpg, 2004.

Geographical Survey Institute, Coseismic horizontal and vertical displacements due to the 2007 Noto Hanto earthquake detected by the continuous GPS observation, http://www.gsi.go.jp/BOUSAI/isikawa/tikaku.htm, 2007 (in Japanese).

Geological Survey of Japan, *1:200,000 scale geological map of Nanao and Toyama regions*, 1967.

Geological Survey of Japan, *1:1,000,000 scale geological map of Japan, third edition*, 1992.

Earthquake Research Committee of the Headquarters for Earthquake Research Promotion, *National seismic hazard map for Japan*, 121 pp., 2005.

Hodgkinson, K. M., R. S. Stein, K. W. Hudnut, J. Satalich, and H. Richards, Damage and restoration of geodetic infrastructure caused by the 1994 Northridge, California, earthquake, U. S. Geological Survey Open-File Report #96-517, http://geopubs.wr.usgs.gov/open-file/of96-517/fema/html/FEMA.html, 1996.

Japan Meteorological Agency (JMA), CMT solution of the March 25, 2007 Noto Hanto Oki M 6.9 earthquake, http://www.seisvol.kishou.go.jp/eq/mech/cmt/fig/cmt20070325094157.html, 2007 (in Japanese).

Katagawa, H., M. Hamada, S. Yoshida, H. Kadosawa, A. Mitsuhashi, Y. Kono, and Y. Kinugasa, *J. Geogr.*, **114**, 791–810, 2005 (in Japanese with English abstract).

Matsuda, T., Magnitude and recurrence interval of earthquakes from a fault, *Zisin, Ser. 2*, **28**, 269–283, 1975 (in Japanese with English abstract).

National Research Institute for Earth Science and Disaster Prevention, Earthquake mechanism information of the March 25, 2007 Noto Hanto earthquake, http://www.fnet.bosai.go.jp/freesia/event/tdmt/20070325091000/update2/index.html, 2007.

Okada, Y., Expected crustal deformation due to seismic faulting, *Programme and abstracts, the Seismological Society of Japan, 1992, fall meeting*, **240**, 1992 (in Japanese).

Okamura, Y., Explanatory notes of geological map west of Noto Peninsula 1:200,000, *Marine Geology Map series*, **61** (CD), Geological Survey of Japan, AIST, 2003.

Okumura, K., The grey zone of the active faulting, Tottori, Niigata, Bam, and Kobe-un essai, *Abstracts of the Hokudan International Symposium on Active Faulting*, 114–116, 2005.

Ota, Y., Late Quaternary vertical movement in Japan estimated from deformed shorelines, *Roy. Soc. N. Z. Bull.*, **13**, 231–239, 1975.

Ota, Y. and K. Hirakawa, Marrine terraces and their deformation in Noto Peninsula, Japan Sea side of central Japan, *Geogr. Rev. Jpn.*, **52**(4), 169–189, 1979 (in Japanese with English abstract).

Ota, Y., T. Matsuda, and J. Hirakawa, Active faults in Noto Peninsula, central Japan, *Quatern. Res.*, **15**, 109–128, 1976 (in Japanese with English abstract).

Ota, Y., T. Sekiguchi, M. Taguchi, K. Yoshitake, and S. Odagiri, 1:100,000 scale map and explanatory (pp. 16) of crustal movement and land condition map of Noto Peninsula, http://www1.gsi.go.jp/geowww/themap/pdf/disa-pdf/d1347.pdf, 1998.

Research Group for Active Faults in Japan, *Active Faults in Japan, sheet maps and inventories, rev. ed.*, 437 pp., Univ. of Tokyo Press, Tokyo, 1991.

Sagiya, T., S. Miyazaki, and T. Tada, Continuous GPS array and present-day crustal deformation of Japan, *Pure Appl. Geophys.*, **157**, 2302–2322, 2000.

Schwartz, D. P. and K. J. Coppersmith, Fault behavior and characteristic earthquakes: Examples from the Wasatch and San Andreas fault zones, *J. Geophys. Res.*, **89**, 5681–5698, 1984.

Stein, R. S. and G. Ekstrom, Seismic and geometry of a 110-km-long blind thrust fault 2. Synthesis of the 1982–1985 California earthquake sequence, *J. Geophys. Res.*, **97**, 4865–4883, 1992.

Toda, S., Coulomb stresses imparted by the 25 March 2007 $M_w = 6.6$ Noto-Hanto, Japan, earthquake explain its 'butterfly' distribution of aftershocks and suggest a heightened seismic hazard, *Earth Planets Space*, **60**, this issue, 1041–1046, 2008.

USGS, Magnitude 6.7—near the west coast of Honshu, Japan 2007 March 25 00:41:57 UTC, http://earthquake.usgs.gov/eqcenter/eqinthenews/2007/us2007aiae/, 2007.

Wallace, R. E., Earthquake recurrence intervals on the San Andreas fault, *Geol. Soc. Am. Bull.*, **81**, 2875–2890, 1970.

Wells, D. L. and K. J. Coppersmith, New empirical relationships among magnitude, rupture length, rupture width, rupture area, and surface displacement, *Bull. Seismol. Soc. Am.*, **84**, 974–1002, 1994.

S. Toda (e-mail: s-toda@aist.go.jp) and Y. Awata